Chinese Journal of Physiology 53(6): 430-438, 2010
DOI: 10.4077/CJP.2010.AMM027

Fine Frequency-Modulation Trigger Features of Midbrain Auditory Neurons Extracted by the Progressive Thresholding Method — A Preliminary Study

T.R. Chang[1], T.W. Chiu[2], X. Sun[3], and Paul W.F. Poon[4]

[1]*Department of Computer Sciences and Information Engineering, Southern Taiwan University Tainan, Taiwan, ROC*
[2]*Department of Biological Science and Technology, National Chiao Tung University Hsinchu, Taiwan, ROC*
[3]*Division of Life Sciences, East China Normal University, Shanghai, PRC*
and
[4]*Department of Physiology, Medical College, National Cheng Kung University Tainan 70101, Taiwan, Republic of China*

Abstract

Spectro-temporal receptive fields (STRFs) are commonly used to characterize response properties of central auditory neurons and for visualizing 'trigger features'. However, trigger features in STRF maps typically have a blurry appearance. Therefore it is unclear what details could be embedded in them. To investigate this, we developed a new method called 'progressive thresholding' to resolve fine structures in the STRFs, and applied the method to FM responses recorded from single units at the auditory midbrain of anesthetized rats. Random FM tones of a narrow frequency range (~0.5 octave) were first presented to evoked spike responses at the cell's best frequency. Perispike modulating time waveforms collected (50 msec long, n = 1,500 to 4,000 tracings) were used to generate STRF based on spike-triggered-averaging. After supra-threshold areas of pixel counts had been determined through a step of progressive thresholding in the map, those peri-spike modulating waveforms passing through each area were dejittered systematically. At what seemed to be an optimal threshold, multiple trigger features (up to a maximum of 4 fine bands) were extracted from the initially simple-looking STRF. Results show that fine FM trigger features are present in STRFs and that they can be resolved with the present method of analysis.

Key Words: inferior colliculus, FM, STRF, component trigger feature

Introduction

In many natural sounds, the energy pattern seldom appears constant but changes with time. Frequency modulation (FM) represents one of such fundamental time variances in sound energy (16). Many central auditory neurons develop great sensitivity to FM sounds compared with steady tones ('FM-sensitive' cells) (22, 31, 38, 46). These neurons emerge in substantial numbers first at the level of the midbrain and more of them are found in the cortex (18, 22, 30, 34, 38, 41). Most of these neurons discharge spikes in response to specific spectro-temporal patterns of energy embedded in the stimulating sounds (or for simplicity we called them 'FM trigger features'). Since complex sounds like speech contain

Corresponding author: Dr. Paul W.F. Poon, Department of Physiology, Medical College, National Cheng Kung University, 1 University Road, Tainan 70101, Taiwan, Republic of China. Fax: +886-6-2362780, E-mail: ppoon@mail.ncku.edu.tw
Received: November 12, 2009; Revised: February 13, 2010; Accepted: February 24, 2010.
 ISSN : 0304-4920. http://www.cps.org.tw

similar time-varying signals, the importance of neural mechanisms of FM coding is often related to the recognition of complex sounds including speech in humans (4, 12, 39, 42).

Different approaches have been developed to determine trigger features of FM-sensitive neurons, typically in terms of their receptive fields or commonly known as the 'spectral temporal receptive field' (STRF) (2, 14). In spite of the differences in methodology used across laboratories to obtain STRFs, the main spirit of the approach remains the same, *i.e.*, a somewhat randomly structured sound (*e.g.*, dynamic ripple noise, random chords, random FM tone, naturally occurring or even vocalization sound) is presented to the animal to evoke spike activity recorded from a micro-electrode placed near the cell. Datasets containing the peri-spike stimulus energy are then processed with spike-trigger-averaging or reverse correlation analysis to yield the STRF on the perispike-time-vs-frequency plane with the intensity of stimulus energy typically represented in a temperature color-code (1, 15, 17, 26, 29, 33, 40, 43). For a given cell, the appearance of STRF is often stimulus-dependent (47) and can undergo plastic changes (19). In most STRFs so determined, the trigger features appear rather blurry (7, 13, 19, 44, 47, 48). This blurred appearance is partly due to that fact that when spike times are aligned to generate the STRF, and consequently spike response jitter is artificially transferred to time jitter in the trigger feature. In the presence of multiple trigger features, their overlaps in the STRF may also blur the features. Limited attempts have been made with some success to sharpen the trigger feature using a variety of dejittering algorithms (3, 8, 20). No attempt has yet been made to reveal finer structures, or to determine if there is any present in the STRF.

This study is aimed to implement a method to determine if fine trigger features exist in the STRF. In brief, the method performs spike dejittering based on a series of potential trigger features extracted through a progressive thresholding of pixel counts in the map. We applied the method to simple-looking STRFs collected from midbrain auditory neurons. Preliminary results revealed striking details of fine trigger features that were not evident in the original STRFs.

Materials and Methods

Animal Preparation

Rats (Sprague Dawley, 200-250 gm, n = 5) were anesthetized with urethane (1.5 g/kg, i.p., maintained at 0.4 g/kg for pain areflexia when necessary) and fixed with a special head holder for recording extracellular single spike activities using conventional electrophysiological procedures (details see Ref. 32). The skull overlying the occipital cortex was surgically opened and glass micropipette electrode (20-70 MΩ, 3M KCl filled) advanced into the midbrain (inferior colliculus) using a stepping micro-drive (Narishige) to hunt for single units that would respond to repetitive clicks (0.1 msec pulse, ~90 dB SPL). After conventional amplification, filtering and conditioning (Axonprobe 1A, PARC-5113), unit responses to sounds were recorded for off-line analysis.

Acoustic Stimulation

The random FM tones were generated by digitally low-pass filtering a white noise at 12.5, 25 or 125 Hz. The filtered signal was then fed to a function generator (Tektronix FG280) at its voltage-control-frequency input to control the instantaneous frequency of a continuous tone. The resultant stimulus was a continuous FM signal with frequency randomly varied over time (such signal is powerful stimulus for auditory neurons in the rat midbrain (Ref. 30, 33). After determining the unit's most sensitive frequency (or best frequency, BF), the center frequency of the FM tone was set at this BF with a modulation range of ~0.5 octave. Stimulus intensity was set ~30 dB suprathreshold at the BF. We first collected spike responses at a fixed carrier frequency with all the 3 sets of FM tones, and only the one producing the maximal spike count was used for subsequent data analysis. Each spike dataset was a continuous recording of 2 min, and to increase sample size the dataset collection was repeated up to a maximum of 5 datasets for individual units.

Electrophysiology

A computer interface (Tucker Davies Technology System II Alachua, FL, USA) was programmed to deliver the modulating waveforms while simultaneously collecting spike responses at 2 kHz (spikes pre-conditioned into 0.4 msec pulses). Details of the recording procedures can be found in earlier publications (32). During experiment, the animal was placed inside a sound-treated chamber (Industrial Acoustic Company) for free-field acoustic stimulations, and its normal body temperature was maintained with a servo-control heating pad. The procedure was approved by the Animal Ethics Committee, Laboratory Animal Center, NCKU.

Data Analysis

To extract fine trigger features, a special method called for simplicity the 'progressive thresholding

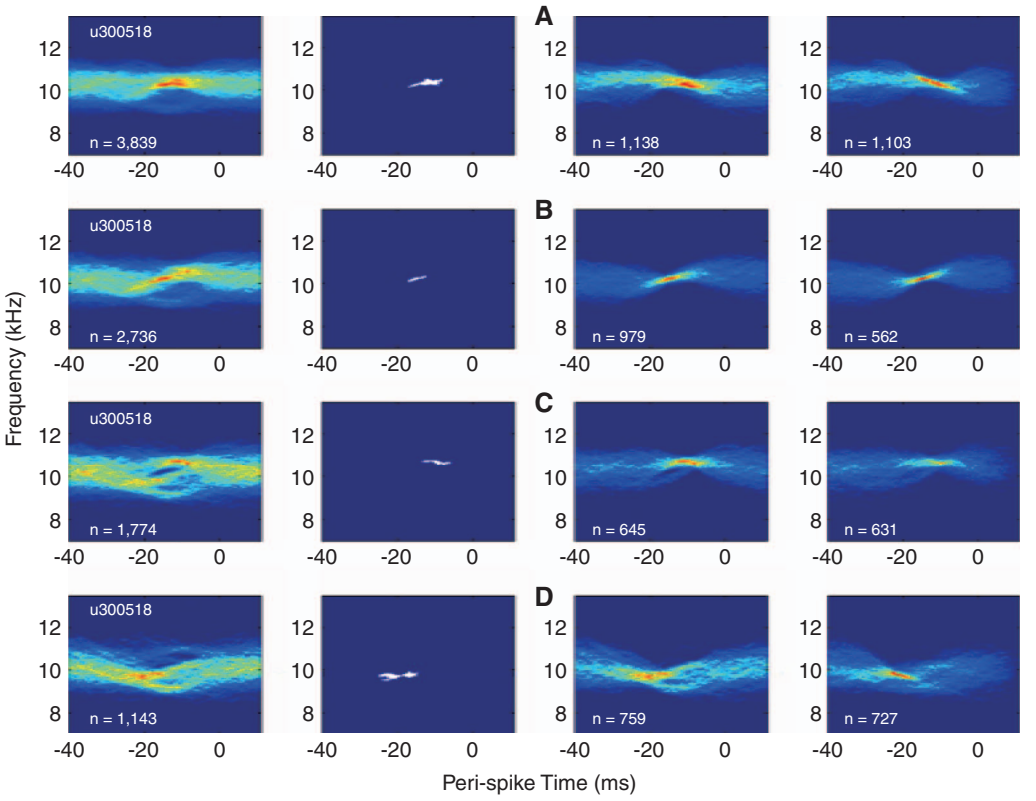

Fig. 1. STRFs of an FM-sensitive cell showing the successive extractions of fine trigger features through 4 cycles of successive thresholding (from top to bottom rows, at 75% of the current peak count). Left column: STRFs before processing of each cycle; second column: supra-threshold areas (white) identified; third column: STRFs formed by the tracings passing through the supra-threshold areas before dejittering; right column: component STRFs after dejittering. Note (**B**) to (**D**) represent the tracings before entering the cycle of processing and include all tracings not used in the component STRFs from previous cycles. For this cell, 4 component STRFs (each with n > 150 tracings) are generated to be combined later into a composite map (Fig. 3**I**). In this and other figures, a temperature code is used to represent pixel counts in the STRF maps (warm colors high, cold colors low). Spikes occur at time zero, with minus representing pre-spike time. Unit identifier is shown on left-upper corner, and 'n=' is number of peri-spike tracings used in the corresponding panels.

method' was used to analyze the collected datasets. It consisted of the following steps and was conducted using a tailor-made MATLAB program:

1. Generating the original STRF: For a given unit, multiple datasets collected at a single carrier frequency of the FM tone were first combined into one dataset. The result was plotted on the spectral temporal plane to show the distribution of the peri-spike modulating time waveform. Like conventional STRF maps, pixel counts were color-coded to visualize trigger features (Fig. 1A). To facilitate data analysis, the spatial noise in the original STRF was suppressed using a spatial filter.
2. Finding potential trigger features: at a fractional level of the maximal pixel count (starting at 55%), pixels with counts equal to or greater than the threshold level were identified and outlined as a 'supra-threshold area' (a procedure that is equivalent to slicing the top pixel counts in the map; Fig. 1B). Usually one area was detected. In the case of detecting more than one area, the one larger in size was processed first.
3. Screening peri-spike modulating waveforms: time tracings of modulating waveforms passing through the supra-threshold areas were extracted (Fig. 1C).
4. Dejittering: a dejitter algorithm (details see Ref. 9) was applied to adjust time variance in spike response related to the selected tracings to yield a sharpened 'component STRF' (Fig. 1D). Tracings failed to be dejittered were returned to the original dataset for next round processing. To extract reliable features, we set a criterion of a minimum tracings (n > 150) in order to represent the results as a component STRF. Tracings of those STRFs that failed to meet this criterion were also returned to the original dataset for next round processing.
5. In the case of more than one supra-threshold areas, steps 3 to 4 were repeated for each area.
6. 'Progressive thresholding': we then reapplied the

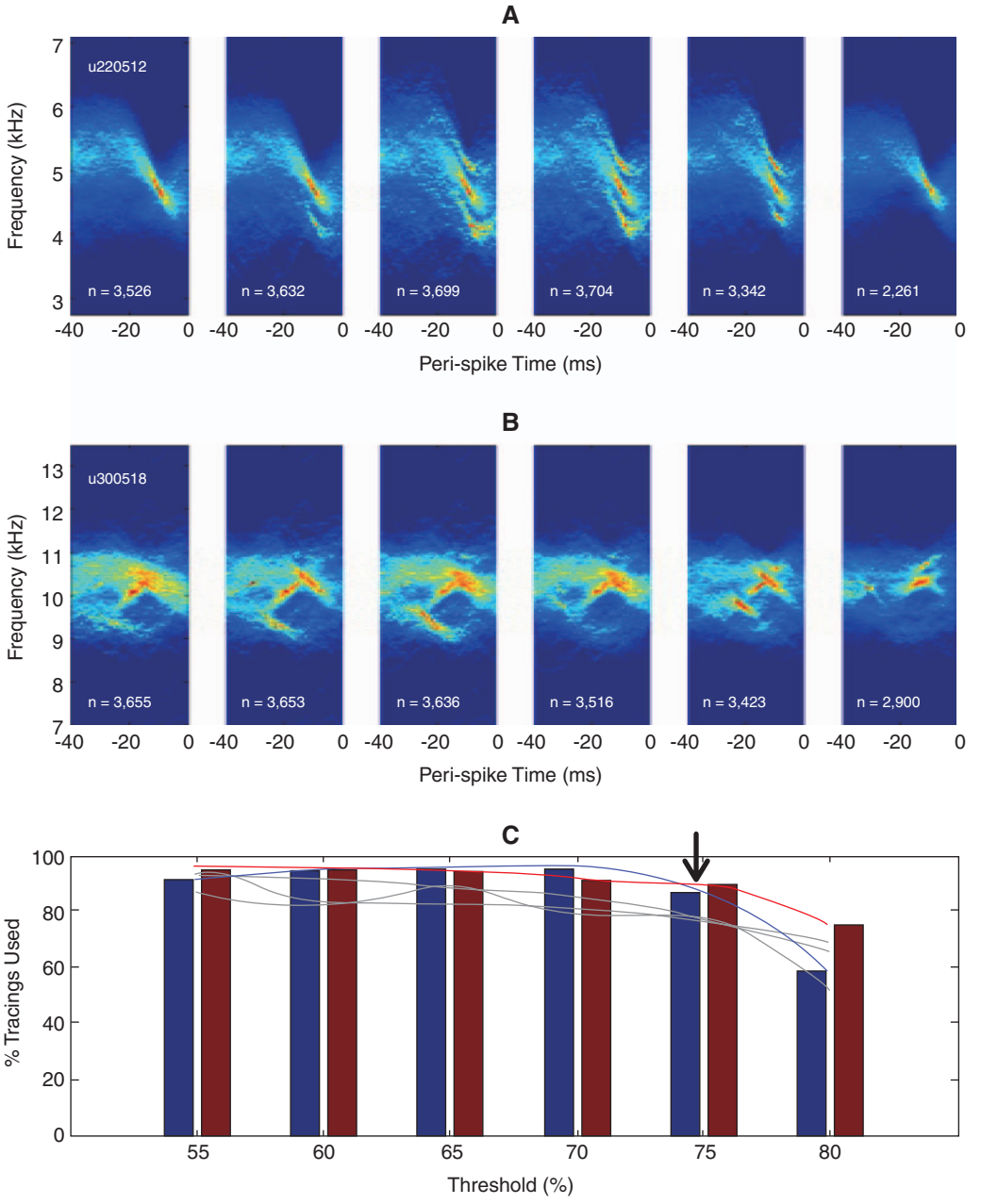

Fig. 2. (**A**), (**B**): Examples of composite STRFs from two cells generated at 6 different thresholds (55% to 80% at 5% steps, from left to right columns). Note that the fine features extracted 'evolves' across thresholds from low to high, reaching an apparently most complex appearance around 75% threshold, where the number of trigger features is also the highest (second column from the right). (**C**): The relationship between percentage tracings used in the composite STRF maps and the threshold is depicted in bar chart for the two cells shown in **A** and **B**, with their optimal thresholds marked by an arrow. The relationship is also shown as fitted curves (3rd order polynomial) for these two FM-sensitive units (color lines) and 3 more others (grey lines).

process of thresholding to the map formed by the remaining tracings. Steps 2 to 5 were repeated to produce additional component STRFs (Fig. 1, E-P).

7. Producing the 'composite STRF': to facilitate viewing of multiple trigger features in the same map, the peak pixel count in each component STRF was first normalized. The component STRFs were then combined into one map through the maximum projection algorithm (*i.e.*, at each pixel position of the composite map, its value was the maximum value at the same pixel determined across component STRFs; Fig. 2, A and B). This composite STRF represents the final result obtained at a particular threshold.
8. Starting with a new threshold value, steps 2 to 7

Table 1. Some unit statistics on the extraction of fine trigger features using the 'progressive thresholding' method (n = 5 FM-sensitive cells)

Parameter	Average	Range
Best frequency of cell	6.5 kHz	2.9 - 10.9 kHz
Number of total tracings analyzed/cell	3,296	1,784 - 3,874
Proportion of tracings rejected by method/cell	14.5%	10.8 - 24.6%
Optimal threshold for fine feature extraction	72%	65 - 75%
Total frequency range of extracted features	0.25 octave	0.1 - 0.41 octave

were repeated (increment step: 5%, up to 80%). For each unit, a total of 6 threshold-dependent composite STRFs were generated (Fig. 2, A and B).

9. Generating 'percentage tracings versus threshold' function': the percentage of tracings used (y) as a function of the corresponding thresholds (x) was then generated (Fig. 2C).
10. Determining the 'optimal threshold': we detected the point of abrupt drop in the function to mark the optimal threshold (Fig. 2C arrow). The composite STRF obtained at the threshold just prior to the abrupt drop was taken to represent the most likely trigger features for the cell (see elaboration later in the Discussion and Fig. 4).

Results

Results from a limited number of FM-sensitive cells showed the effectiveness of the method. Some key statistics of the units are summarized in Table 1. These cells all responded to stimulation with FM but not pure tones (they are called 'FM-specialized cells' according to our previous nomenclature, see 33). With our random FM stimuli, trigger features in the map were discerned as 'hot spot' or a single patch of 'warm' modulating waveforms occurring at about 10 to 20 msec preceding the spike. Consistent with previous reports, such FM bands are basically characterized by 2 stimulus parameters: (a) the optimal rate of frequency modulation (inclusive of the upward or downward direction of frequency sweep), and (b) the optimal range of frequency change. Findings are consistent with FM responses reported at the auditory midbrain (22, 33, 37, 46).

A variety of fine trigger features were revealed in the composite STRFs. These features appeared more discernible or sharper than those in the original maps. In the composite STRFs we found the number of features varied from 1 to 4 across different units (Fig. 3 middle column). The multiple trigger features for a given unit can orient in the same or different directions in the map (representing up- or down-frequency sweeps). The spectro-temporal positions of the multiple features coincide with those warm patches in the original STRFs.

In the STRFs formed by the remaining tracings that were excluded in the final maps, other features were also seen. The proportion of tracings excluded in the final maps was <25% (average: n = 546, range: 193 - 902 or 14.5% of total tracings/unit, range: 10.8 - 24.6%). These tracings represented likely either spontaneous activities (as 3 of the 5 units were spontaneously active), or weak trigger features not detected by the method. In some cases, particularly with units showing no spontaneous activity, the pre-spike modulating time waveforms detoured discrete areas in the map, giving the impression of empty 'holes' untouched by the stimulus energy (Fig. 3, K-L). The boundary of these holes matched well with those of the fine trigger features in the same cell. In other cases, these tracings aggregated in somewhat elongated shapes, appearing as warm patches in the STRF (Fig. 3, M-O). They could reflect some weaker trigger features.

Although the BFs of these cells fall within middle to low frequency ranges, similar examples though fewer were also found in high frequency regions (data not shown). The fact that we found more of these examples in the low and middle frequency ranges could be partly related to the limited dynamic range of the analog tone generator we used to produce the FM sound.

Discussion

Results from our limited sample showed that the progressive thresholding method can extract details of FM trigger features from initially simple-looking STRFs. Algorithms of spike jitter adjustment have been implemented by other investigators to sharpen trigger features (usually on cells with a simple-looking STRFs), but none has yet achieved the present level of fine resolutions. This sensitive method is potentially useful for examining activity- or task- driven synaptic changes occurring in the brain, as they have been reported at the auditory midbrain and in the cortex of mammals and birds (5, 21, 35).

The complexity of fine component features found

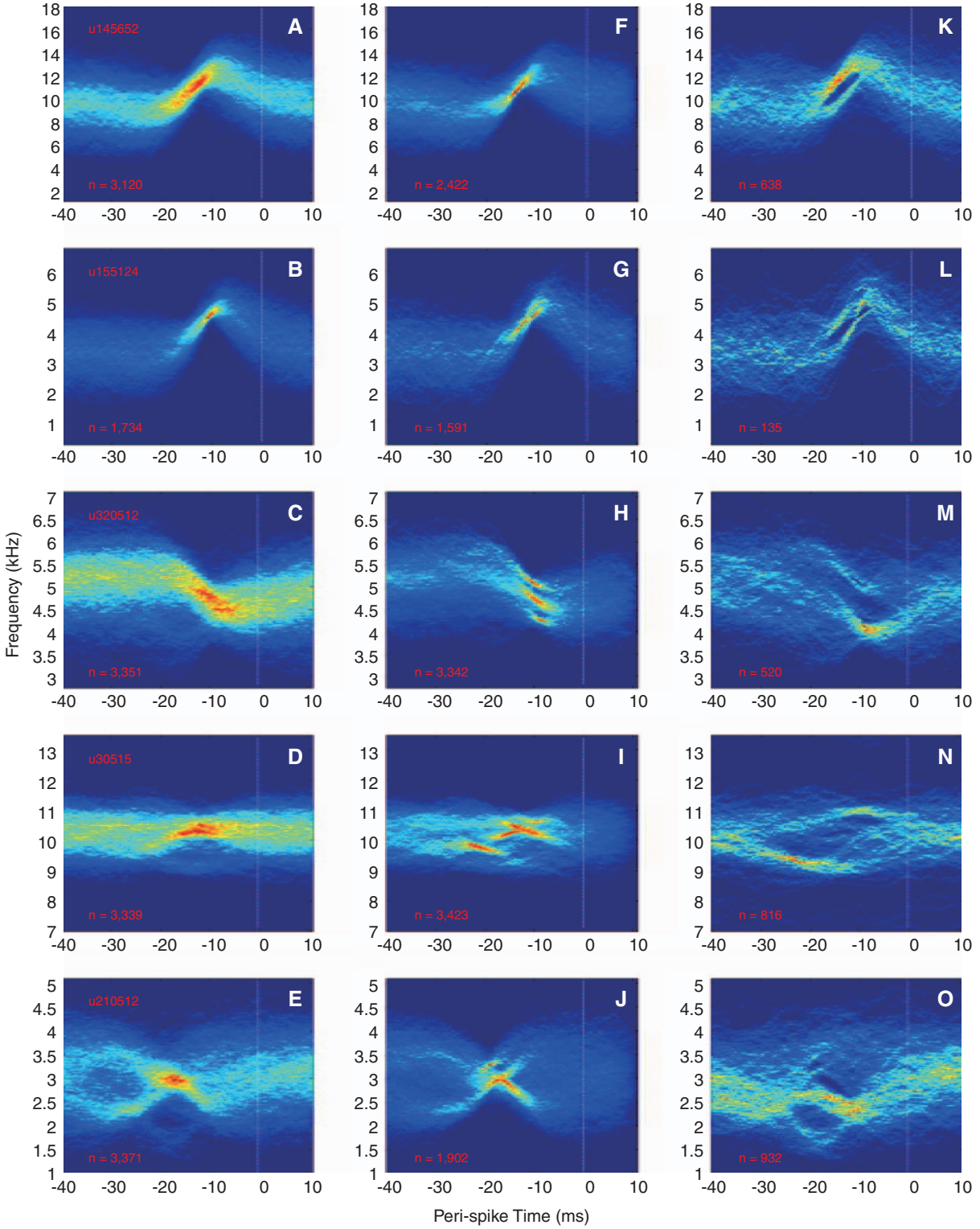

Fig. 3. Results of progressive thresholding are shown for 5 FM-sensitive cells (each row represents a unit). Left column (**A**-**E**): original STRFs; middle column (**F**-**J**): composite STRFs at the optimal threshold; right column (**K**-**O**): STRFs formed by remaining tracings (as excluded by the method). Note details of features extracted (middle column) compared to the original maps (left column) and complementary features in the maps of the residual tracings (right column).

here are in line with other studies reported complex excitatory and inhibitory interactions and non-linear response properties at the auditory midbrain (13, 23, 24, 28). Fine trigger features appeared within a narrow frequency range (average: 0.25 octave), a finding that is likely related to the narrow frequency

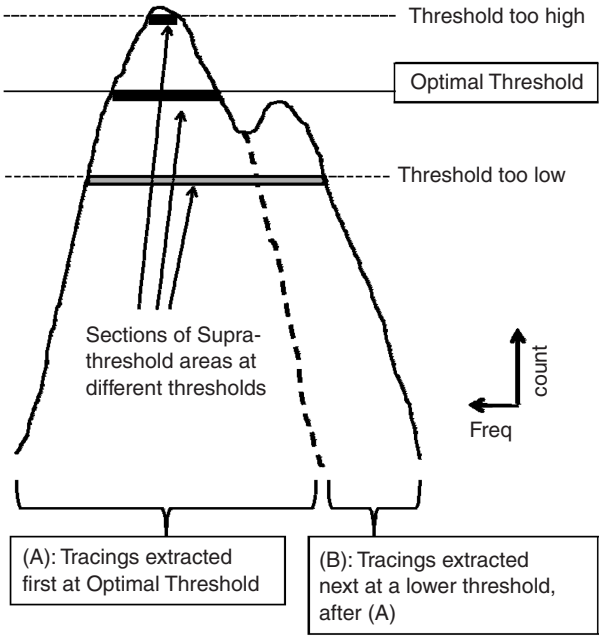

Fig. 4. A schematic diagram to illustrate the idea of the 'optimal threshold'. The two-peak pixel count profile represents a vertical cross-section through the STRF showing a hypothetical situation of one major and one minor trigger features running in the same direction (*e.g.*, like the situation depicted in **Fig. 2A**, second panel from the left). At the optimal threshold (*e.g.*, 75%), only the major (taller) peak is detected as supra-threshold, and its associated tracings are extracted into a component STRF after dejittering. In the next cycle of processing, the threshold is lowered (since it is taking 75% of whatever peak counts left in the map after removal of the taller peak), and the minor (shorter) peak becomes prominent and is now detected as supra-threshold. The component STRF will be generated by the method in the absence of interference of the previous major peak. If the threshold is set too low (*e.g.*, 55%), both peaks will be included and the method fails to separate them into different features (*e.g.*, **Fig. 2A**, left-most panel). If the threshold is set too high (e.g., 80%), too many tracings are excluded, resulting in a smaller trigger area (*e.g.*, **Fig. 2A**, right-most panel) and a drop in the number of tracings (**Fig. 3C**).

scan we had used (~0.5 octave). The spectral range of ~0.25 octave can be taken to reflect integration of neural activities within 'single' frequency lamina in the midbrain (11, 25) or even on individual dendrites of the FM-sensitive cells, which have large dendritic field with complex dendritic morphology (30). The finding of multiple fine trigger features is also consistent with earlier reports on FM-sensitive cells, showing that in STRFs with simple-looking trigger feature, partial or component-like features can sometimes be observed using a different method of analysis based on jitter adjustment times (8). Related to this finding, multiple trigger features have been reported in the STRFs of midbrain auditory neurons when stimulated with FM tones of broad spectrum (10).

The possibility nevertheless exists that the multiple fine trigger features so revealed could be artifacts. Firstly, despite some parameters in the method is determined in a data-driven manner (*e.g.*, the 'optimal threshold'), observed results could be distorted by inappropriate setting of parameters in our method. The rationale of choosing the important parameter of the optimal threshold is elaborated as follows. Fig. 4 illustrates diagrammatically what might have happened when two hypothetical trigger features in the original STRF are processed at different thresholds. It is conceivable that at too low a threshold, the supra-threshold area (a potential trigger feature) would be larger than what is occupied in the map by the true trigger feature. This enlarged supra-threshold area would likely result in merging two nearby trigger features into one during the dejitter process (particularly when they are in the same direction of modulation). Tracings unrelated to the true trigger features could also be included, resulting in blurred trigger features. Our results on composite STRFs obtained across a range of thresholds (Fig. 2, A and B) provided evidence in support of such possibilities. Only at the optimal threshold, two trigger features of different strengths will be sliced between their peaks. This allows the method to separate them into two trigger features (regardless of their FM directions). At thresholds that are too high, the true trigger areas shrink, and increasingly more tracings related to the trigger feature are excluded, resulting in a drop in the percentage of tracings used to produce the final map. How fast and deep the drop on the function appears likely depends on how steep the peak of pixel count rises from the map. The observation that composite STRFs extracted below the optimal threshold remained relatively stable over a range (Fig. 2, A and B) supports the above argument. Validity of the method would still need to be examined in future experiments that are designed to predict neural responses precisely in the same cell based on the fine trigger features, and to test the method with simulated datasets of STRF where trigger structures are predetermined and the ground truth known. Secondly, we could have recorded from multiple instead of single units. These spikes we believe most likely belonged to single units since waveforms of extracellular action potentials recorded with our sharp micropipettes were rather stereotyped with large spike amplitudes (typically 10 to 20 times the background noise level).

One needs to point out that the current method made a few assumptions on the response of the cell. First, the trigger features are time-invariant (at least over the ~10 min of data collection), and therefore it

is justified to combine datasets to provide enough spikes for processing. Our consistent STRFs obtained by processing datasets from the same unit across time supported that the trigger features were relatively stable at least within 10 min. Second, the fine trigger features are packed in the time-vs-frequency plane with gaps resolvable using our spectral and temporal sampling intervals (0.008 to 0.023 octave, 0.5 msec). The present results would need to be confirmed by experiments using finer sampling intervals. Third, each trigger feature was associated with a sufficiently large number of spikes for the generation of discernible component features. The method did sometimes fail to work, particularly with tracings fewer than 100. The limit of $n > 150$ tracings was empirically set to avoid over-estimating trigger features. But the limit needs to be determined more systematically.

In most of the spike-trigger averaging approach, it was assumed implicitly that spikes were generated as a result of cell excitation, whereas the role of inhibition and other properties of the cell remain unclear. Our previous study (8) suggested that spikes evoked by random FM stimulation could be generated by multiple mechanisms. In the present experiment, some preliminary evidence in support of heterogeneity of spike origin was also found in the dejitter-time histograms. Specifically, the dejitter time histograms of a given cell can be one that resembles the normal spike PSTH with a fast rising phase and a slow falling phase for a component feature, or the time-reversed PSTH of the first kind (data not shown). Results are in line with the known complex interaction between excitatory and inhibitory synaptic actions in the auditory midbrain, inhibitory region in the STRF and the nonlinear properties of neural circuit in response to sounds (6, 12, 27, 36, 42, 45). Further experiments with intra-cellularly recordings from FM-sensitive cells would certainly help to clarify this conjecture.

Our random FM stimulation using a single tone has the advantage of its simplicity because stimulus energy is narrowly channeled to the cell. Some information of cell's response could however be missing. For example inhibitory regions in the STRF and interactions among different tone components are not revealed (especially in the absence of spontaneous activity), unlike approaches using dynamic ripple, random chords or natural sounds as stimuli. Prediction of cells responses to complex sounds has recently been modeled with remarkable fidelity based on functional grouping of STRFs across populations (48). It would be interesting to compare modeling results based on populations with results based on single neurons (like the present one). Perhaps a combined approach using different stimulus sets to collect responses from a single neuron would help further understanding of coding mechanisms of complex sounds.

Acknowledgments

Supported in part by National Science Council, Taiwan 98-2221-E-218-039.

References

1. Aertsen, A.M. and Johannesma, P.I. The spectro-temporal receptive field. A functional characteristic of auditory neurons. *Biol. Cybern.* 42: 133-143, 1981.
2. Aertsen, A.M. and Johannesma, P.I. A comparison of the spectro-temporal sensitivity of auditory neurons to tonal and natural stimuli. *Biol. Cybern*. 42: 145-156, 1981.
3. Aldworth, Z.N., Miller, J.P., Gedeon, T., Cummins, G.I. and Dimitrov, A.G. Dejittered spike-conditioned stimulus waveforms yield improved estimates of neuronal feature selectivity and spike-timing precision of sensory interneurons. *J. Neurosci*. 25: 5323-5332, 2005.
4. Andoni, S., Li, N. and Pollak, G.D. Spectrotemporal receptive fields in the inferior colliculus revealing selectivity for spectral motion in conspecific vocalizations. *J. Neurosci*. 27: 4882-4893, 2007.
5. Bergan, J.F. and Knudsen, E.I. Visual modulation of auditory responses in the owl inferior colliculus. *J. Neurophysiol*. 101: 2924-2933, 2009.
6. Bieser, A. Processing of twitter-call fundamental frequencies in insula and auditory cortex of squirrel monkeys. *Exp. Brain Res*. 122: 139-148, 1998.
7. Britvina, T. and Eggermont, J.J. Spectrotemporal receptive fields during spindling and non-spindling epochs in cat primary auditory cortex. *Neurosci*. 154: 1576-1588, 2008.
8. Chang, T.R., Chiu, T.W., Chung, P.C. and Poon, P.W. Should spikes be treated with equal weightings in the generation of spectro-temporal receptive fields? *J. Physiol. (Paris)* 104: 215-222, 2010.
9. Chang, T.R., Chung, P.C., Chiu, T.W. and Poon, P.W. A new method for adjusting neural response jitter in the STRF obtained by spike-trigger averaging. *Biosystems* 79: 213-222, 2005.
10. Chiu, T.W. and Poon, P.W. Multiple-band trigger features of midbrain auditory neurons revealed in composite spectro-temporal receptive fields. *Chinese J. Physiol*. 50: 105-112, 2007.
11. Clopton, B.M. and Winfield, J.A. Tonotopic organization in the inferior colliculus of the rat. *Brain Res*. 56: 355-368, 1973.
12. Cohen, Y.E., Theunissen, F., Russ, B.E. and Gill, P. Acoustic features of rhesus vocalizations and their representation in the ventrolateral prefrontal cortex. *J. Neurophysiol*. 97: 1470-1484, 2007.
13. David, S.V., Mesgarani, N., Fritz, J.B. and Shamma, S.A. Rapid synaptic depression explains nonlinear modulation of spectro-temporal tuning in primary auditory cortex by natural stimuli. *J. Neurosci*. 29: 3374-3386, 2009.
14. deCharms, R.C., Blake, D.T. and Merzenich, M.M. Optimizing sound features for cortical neurons. *Science* 280: 1439-1443, 1998.
15. Depireux, D.A., Simon, J.Z., Klein, D.J. and Shamma, S.A. Spectrotemporal response field characterization with dynamic ripples in ferret primary auditory cortex. *J. Neurophysiol*. 85: 1220-1234, 2001.
16. Doupe, A.J. and Kuhl, P.K. Birdsong and human speech: common themes and mechanisms. *Ann. Rev. Neurosci*. 22: 567-631, 1999.
17. Escabi, M.A. and Schreiner, C.E. Nonlinear spectrotemporal sound analysis by neurons in the auditory midbrain. *J. Neurosci*. 22: 4114-4131, 2002.

18. Felsheim, C. and Ostwald, J. Responses to exponential frequency modulations in the rat inferior colliculus. *Hearing Res*. 98: 137-151, 1996.
19. Fritz, J., Shamma, S., Elhilali, M. and Klein, D. Rapid task-related plasticity of spectrotemporal receptive fields in primary auditory cortex. *Nature Neurosci*. 6: 1216-1223, 2003.
20. Gollisch, T. Estimating receptive fields in the presence of spike-time jitter. *Network* 17: 103-129, 2006.
21. Grana, G.D., Billimoria, C.P. and Sen, K. Analyzing variability in neural responses to complex natural sounds in the awake songbird. *J. Neurophysiol*. 101: 3147-3157, 2009.
22. Heil, P., Rajan, R. and Irvine, D.R. Sensitivity of neurons in cat primary auditory cortex to tones and frequency-modulated stimuli. I: Effects of variation of stimulus parameters. *Hearing Res*. 63: 108-134, 1992.
23. Kao, M.C., Poon, P.W.F. and Sun, X. Modeling of the response of midbrain auditory neurons in the rat to their vocalization sounds based on FM sensitivities. *Biosystems* 40: 103-109, 1997.
24. Lesica, N.A. and Grothe, B. Dynamic spectrotemporal feature selectivity in the auditory midbrain. *J. Neurosci*. 28: 5412-5421, 2008.
25. Malmierca, M.S. The inferior colliculus: a center for convergence of ascending and descending auditory information. *Neuroembryol. Aging* 3: 215-229, 2004.
26. Miller, L.M., Escabí, M.A., Read, H.L. and Schreiner, C.E. Spectrotemporal receptive fields in the lemniscal auditory thalamus and cortex. *J. Neurophysiol*. 87: 516-527, 2002.
27. Nagarajan, S.S., Cheung, S.W., Bedenbaugh, P., Beitel, R.E., Schreiner, C.E. and Merzenich, M.M. Representation of spectral and temporal envelope of twitter vocalizations in common marmoset primary auditory cortex. *J. Neurophysiol*. 87: 1723-1737, 2002.
28. Nagel, K.I. and Doupe, A.J. Organizing principles of spectro-temporal encoding in the avian primary auditory area field L. *Neuron* 58: 938-955, 2008.
29. Noreña, A.J., Tomita, M. and Eggermont, J.J. Neural changes in cat auditory cortex after a transient pure-tone trauma. *J. Neurophysiol.* 90: 2387-2401, 2003.
30. Poon, P.W., Chen, X. and Cheung, Y.M. Differences in FM response correlate with morphology of neurons in the rat inferior colliculus. *Exp. Brain Res*. 91: 94-104, 1992.
31. Poon, P.W., Chen, X. and Hwang, J.C. Basic determinants for FM responses in the inferior colliculus of rats. *Exp. Brain Res*. 83: 598-606, 1991.
32. Poon, P.W.F. and Chiu, T.W. Similarities of FM and AM receptive space of single units at the auditory midbrain. *Biosystems* 58: 229-237, 2000.
33. Poon, P.W. and Yu, P.P. Spectro-temporal receptive fields of midbrain auditory neurons in the rat obtained with frequency modulated stimulation. *Neurosci. Lett*. 289: 9-12, 2000.
34. Qi, Y., Casseday, J.H. and Covey, E. Response properties and location of neurons selective for sinusoidal frequency modulations in the inferior colliculus of the big brown bat. *J. Neurophysiol*. 98: 1364-1373, 2007.
35. Rahne, T. and Sussman, E. Neural representations of auditory input accommodate to the context in a dynamically changing acoustic environment. *Eur. J. Neurosci*. 29: 205-211, 2009.
36. Rauschecker, J.P. Compensatory plasticity and sensory substitution in the cerebral cortex. *Trends Neurosci*. 18: 36-43, 1995.
37. Rees, A. and Kay, R.H. Delineation of FM rate channels in man by detectability of a three-component modulation waveform. *Hearing Res.* 18: 211-221, 1985.
38. Rees, A. and Møller, A.R. Responses of neurons in the inferior colliculus of the rat to AM and FM tones. *Hearing Res*. 10: 301-330, 1983.
39. Sen, K., Theunissen, F.E. and Doupe, A.J. Feature analysis of natural sounds in the songbird auditory forebrain. *J. Neurophysiol.* 86: 1445-1458, 2001.
40. Shechter, B. and Depireux, D.A. Stability of spectro-temporal tuning over several seconds in primary auditory cortex. *Neurosci.* 148: 806-814, 2007.
41. Suga, N. Analysis of frequency-modulated and complex sounds by single auditory neurones of bats. *J. Physiol.* 198: 51-80, 1968.
42. Theunissen, F.E., Sen, K. and Doupe, A.J. Spectral-temporal receptive fields of nonlinear auditory neurons obtained using natural sounds. *J. Neurosci*. 20: 2315-2331, 2000.
43. Valentine, P.A. and Eggermont, J.J. Stimulus dependence of spectro-temporal receptive fields in cat primary auditory cortex. *Hearing Res*. 196: 119-133, 2004.
44. Versnel, H., Zwiers, M.P. and van Opstal, A.J. Spectrotemporal response properties of inferior colliculus neurons in alert monkey. *J. Neurosci*. 29: 9725-9739, 2009.
45. Wang, X., Merzenich, M.M., Beiltel, R. and Schreiner, C.E. Representation of a species-specific vocalization in the primary auditory cortex of the common marmoset: temporal and spectral characteristics. *J. Neurophysiol*. 74: 2685-2706, 1995.
46. Whitfield, C. and Evans, E.F. Responses of auditory cortical neurons to stimuli of changing frequency. *J. Neurophysiol*. 28: 655-672, 1965.
47. Woolley, S.M.N., Gill, P.R. and Theunissen, F.E. Stimulus-dependent auditory tuning results in synchronous population coding of vocalizations in the songbird midbrain. *J. Neurosci.* 26: 2499-2512, 2006.
48. Woolley, S.M.N., Patrick, R., Gill, P.R., Fremouw, T. and Theunissen, F.E. Functional groups in the avian auditory system. *J. Neurosci*. 29: 2780-2793, 2009.